

Biallelic Mutations in *MYPN*, Encoding Myopalladin, Are Associated with Childhood-Onset, Slowly Progressive Nemaline Myopathy

Satoko Miyatake,^{1,2,13} Satomi Mitsuhashi,^{3,4,5,13} Yukiko K. Hayashi,^{3,6} Enkhsaikhan Purevjav,⁷ Atsuko Nishikawa,^{3,8} Eriko Koshimizu,¹ Mikiya Suzuki,⁹ Kana Yatabe,⁹ Yuzo Tanaka,⁹ Katsuhisa Ogata,⁹ Satoshi Kuru,¹⁰ Masaaki Shiina,¹¹ Yoshinori Tsurusaki,¹ Mitsuko Nakashima,¹ Takeshi Mizuguchi,¹ Noriko Miyake,¹ Hiroto Saito,^{1,12} Kazuhiro Ogata,¹¹ Mitsuru Kawai,^{9,14} Jeffrey Towbin,⁷ Ikuya Nonaka,³ Ichizo Nishino,³ and Naomichi Matsumoto^{1,*}

Nemaline myopathy (NM) is a common form of congenital nondystrophic skeletal muscle disease characterized by muscular weakness of proximal dominance, hypotonia, and respiratory insufficiency but typically not cardiac dysfunction. Wide variation in severity has been reported. Intranuclear rod myopathy is a subtype of NM in which rod-like bodies are seen in the nucleus, and it often manifests as a severe phenotype. Although ten mutant genes are currently known to be associated with NM, only *ACTA1* is associated with intranuclear rod myopathy. In addition, the genetic cause remains unclear in approximately 25%–30% of individuals with NM. We performed whole-exome sequencing on individuals with histologically confirmed but genetically unsolved NM. Our study included individuals with milder, later-onset NM and identified biallelic loss-of-function mutations in myopalladin (*MYPN*) in four families. Encoded *MYPN* is a sarcomeric protein exclusively localized in striated muscle in humans. Individuals with identified *MYPN* mutations in all four of these families have relatively mild, childhood- to adult-onset NM with slowly progressive muscle weakness. Walking difficulties were recognized around their forties. Decreased respiratory function, cardiac involvement, and intranuclear rods in biopsied muscle were observed in two individuals. *MYPN* was localized at the Z-line in control skeletal muscles but was absent from affected individuals. Homozygous knockin mice with a nonsense mutation in *Mypn* showed Z-streaming and nemaline-like bodies adjacent to a disorganized Z-line on electron microscopy, recapitulating the disease. Our results suggest that *MYPN* screening should be considered in individuals with mild NM, especially when cardiac problems or intranuclear rods are present.

Nemaline myopathy (NM) is a common form of congenital myopathy that is histologically defined by the presence of nemaline bodies within myofibers.¹ Typical clinical features include proximal-dominant muscle weakness, hypotonia, respiratory insufficiency, and bulbar weakness. It is not usually accompanied by ophthalmoplegia or cardiac dysfunction.² Mutations in genes encoding either a component of thin filament, such as *ACTA1* (MIM: 102610),³ *NEB* (MIM: 161650),⁴ *TPM3* (MIM: 191030),⁵ *TPM2* (MIM: 190990),⁶ *TNNT1* (MIM: 191041),⁷ *CFL2* (MIM: 601443),⁸ and *LMOD3* (MIM: 616112),⁹ or proteins associated with thin filament stability or turnover, namely, *KBTBD13* (MIM: 613727),¹⁰ *KLHL40* (MIM: 615340),¹¹ and *KLHL41* (MIM: 607701),¹² have been shown to cause NM, but the genetic cause remains unknown in 25%–30% of individuals with this disease.¹² The onset of the disease and its symptoms vary even among individuals

with the same gene defect, but most affected individuals have delayed motor milestones and proximal-dominant muscle weakness involving facial muscle.¹³ Intranuclear rod myopathy is a variant of NM in which rod-like inclusions are observed in myonuclei, often seen in the severe infantile form of NM with mutations in *ACTA1*.¹⁴ Here, we present biallelic loss-of-function mutations in *MYPN* (MIM: 608517) in association with childhood-onset, slowly progressive NM with intranuclear rods.

Experimental protocols were approved by the local ethics committees (Yokohama City University School of Medicine for individual 1 and National Center of Neurology and Psychiatry for individuals 2–4). Written informed consent was obtained from all individuals or their parents. Clinical information was obtained from the medical records. The mouse study conformed to protocols approved by the Institutional Animal Care and Use

¹Department of Human Genetics, Yokohama City University Graduate School of Medicine, Yokohama, Kanagawa 236-0004, Japan; ²Clinical Genetics Department, Yokohama City University Hospital, Yokohama, Kanagawa 236-0004, Japan; ³Department of Neuromuscular Research, National Institute of Neuroscience, National Center of Neurology and Psychiatry, Kodaira, Tokyo 187-8551, Japan; ⁴Department of Genome Medicine Development, Medical Genome Center, National Center of Neurology and Psychiatry, Kodaira, Tokyo 187-8551, Japan; ⁵Biomedical Informatics Laboratory, Department of Molecular Life Science, Tokai University School of Medicine, Isehara, Kanagawa 259-1193, Japan; ⁶Department of Pathophysiology, Tokyo Medical University, Shinjuku-ku, Tokyo 160-8402, Japan; ⁷Department of Pediatrics, The Heart Institute, University of Tennessee Health Science Center, Memphis, TN 38103, USA; ⁸Department of Education, Interdisciplinary Graduate School of Medicine and Engineering, University of Yamanashi, Chuo-shi, Yamanashi 409-3898, Japan; ⁹Department of Neurology, National Hospital Organization Higashisaitama Hospital, Hasuda, Saitama 349-0196, Japan; ¹⁰Department of Neurology, National Hospital Organization Suzuka National Hospital, Suzuka, Mie 513-8501, Japan; ¹¹Department of Biochemistry, Yokohama City University Graduate School of Medicine, Yokohama, Kanagawa 236-0004, Japan; ¹²Department of Biochemistry, Hamamatsu University School of Medicine, Hamamatsu, Shizuoka 431-3192, Japan

¹³These authors contributed equally to this work

¹⁴Deceased as of September 23, 2016

*Correspondence: naomat@yokohama-cu.ac.jp

<http://dx.doi.org/10.1016/j.ajhg.2016.11.017>

© 2017 American Society of Human Genetics.

Table 1. Clinical Features of the Studied Individuals

	Individual 1	Individual 2	Individual 3	Individual 4
Ethnicity	Japanese	Japanese	Japanese	Japanese
Gender	female	male	female	male
Age at examination	48 years	35 years	55 years	37 years
Age at onset	25 years	4–5 years	first decade	first decade
<i>MYPN</i> mutations	c.2003delA (homozygous)	c.3076–2A>C (homozygous)	c.1129C>T (homozygous)	c.3169C>T, c.3214C>T
Mutant proteins	p.Asn668Thrfs*25	p.Gly1026Valfs*21, p.Gly1026Asnfs*59, p.Gly1026Leufs*57, p.Gly1026_Gln1077del	p.Arg377*	p.Arg1057*, p.Arg1072*
Consanguinity	+	– ^a	NA	–
Family history	+	–	–	–
Prenatal symptoms	–	–	NA	–
Neonatal-infantile problems	+ (weakness in neck flexor muscle)	–	NA	–
Present Status				
Muscle weakness	severe and diffuse, wheelchair bound, requires assistance in daily life, can move only knees, ankles, and fingers by herself	mild and diffuse	mild to moderate in lower limbs and neck, waddling gait, Gowers' sign	moderate in lower limbs, mild in upper limbs, waddling gait, difficulty climbing stairs, unable to squat
Facial involvement and/or high-arched palate	+	+	NA	+
Ophthalmoparesis	–	NA	NA	–
Excessive drooling	–	NA	NA	–
Contracture	–	–	–	–
Respiratory insufficiency (VC)	– (VC 1.23 L, %VC 39.9%)	NA	NA	– (VC 2.13 L, %VC 84%)
Cardiac problems	hypertrophy	NA	NA	diffuse hypokinesia, EF 52%
Arrhythmia	–	NA	NA	first-degree AVB
Dysphagia	–	NA	NA	–
Intellectual disability	–	–	–	–
Minor dysmorphologies	pectus excavatum	pes cavus	equinus foot, scapulae alatae	–
Serum CK (IU/L)	18 (normal 45–163)	13 (normal 0–40)	26 (normal 40–160)	35 (normal 62–289)
Muscle Pathology				
Nemaline bodies	+	+	+	+
Intranuclear rods	+	–	–	+
Type 1 fiber predominance (>90%)	+	+	+	+

Abbreviations are as follows: NA, not available; +, present; –, absent; VC, vital capacity, EF, ejection fraction; AVB, atrioventricular block; and CK, creatine kinase. ^aConsanguinity was not reported, but the parents are from the same isolated village.

Committee at University of Tennessee Health Science Center.

We identified four individuals with biallelic *MYPN* mutations from four independent families through our study. A clinical summary of the four is presented in Table 1. For individual 1 (V-3 of family 1 in Figure 1A), detailed clinical information is provided in the Supplemental Note. Con-

sanguinity was only identified in the family of individual 1, although the parents (I-1 and I-2 of family 2 in Figure 1A) of individual 2 (II-1 of family 2 in Figure 1A) are from the same isolated village. Individual 1 was reported to have recognized the first symptom of difficulty with climbing stairs in her twenties, but her past history suggests that she had symptoms in her first decade (Supplemental

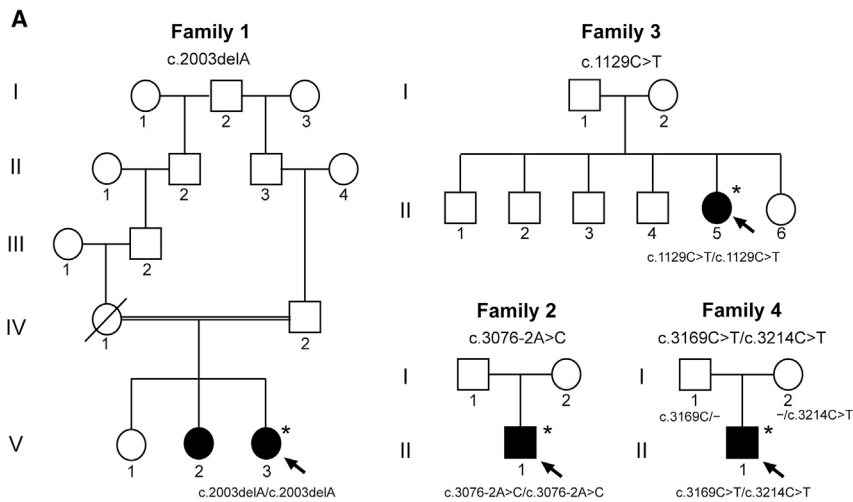
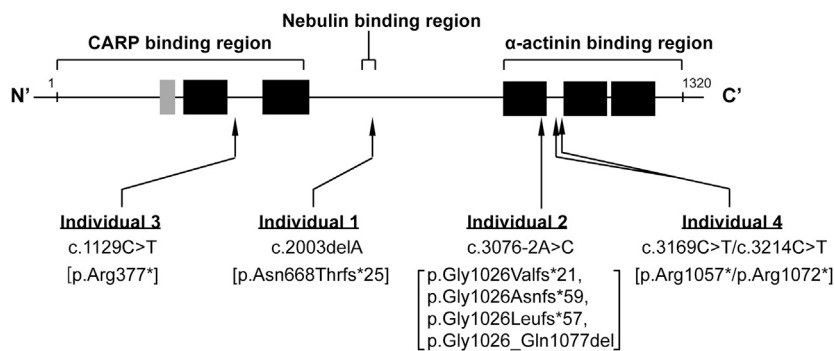


Figure 1. Pedigrees of Families Harboring MYPN Mutations

(A) Families with biallelic MYPN mutations. Black squares and black circles indicate affected male and female individuals, respectively. Arrows indicate probands, and asterisks indicate individuals analyzed by WES. Minus signs indicate that the mutation was not found.

(B) MYPN mutations identified in this study. The upper panel shows a schematic presentation of MYPN structure. Gray and black boxes indicate the coiled-coil domain and Ig domain, respectively. The N-terminal CARP-binding region, nebulin-binding region, and C-terminal α -actinin-binding region are presented. The lower panel shows the positions of the identified mutations along with altered proteins.



Note. Individuals 2, 3 (II-5 of family 3 in Figure 1A), and 4 (II-1 of family 4 in Figure 1A) presented with the initial symptom of gait disturbance during their first decade (around 4–10 years of age). Slowly progressive muscle weakness was first recognized in the extremities, especially the lower limbs, and neck in all four individuals. Facial involvement was observed in individuals 1, 2, and 4 (for whom information on such symptoms is available), and milder signs were observed in individual 1. From the clinical information available (for individuals 1 and 4), extraocular muscles are not involved, and excessive drooling is not present. Three of the individuals can stand up and walk but with some difficulty. Individual 1 (who has the most severe disease) has become wheelchair bound and has required assistance in daily life after her first 15 years of morbidity. Two of the four affected individuals have cardiac problems (cardiac hypertrophy in individual 1 and a diffuse hypokinetic heart with a first-degree atrioventricular block in individual 4). As for respiratory function, two of the four individuals (1 and 4) have decreased vital capacity without apparent respiratory failure. None of the four have dysphagia. Three of the four individuals have minor skeletal dysmorphologies, but none of the four have contractures. Serum creatine kinase is relatively low in all individuals (18, 13, 26, and 35 IU/L in individuals 1, 2, 3, and 4, respectively). All four individuals have normal intelligence.

Muscle computed tomography (CT) was performed on individuals 1 and 4 at the ages of 46 and 35 years, respectively. In individual 4, proximal-dominant muscle atrophy was noted. Atrophy of the neck, gluteal, and femoral muscles was particularly prominent. Interestingly, in the upper legs, the sartorius, gracilis, and biceps brevis femoris muscles were highly degenerated and mostly replaced with fat tissues. Patchy low-density areas were observed especially in semitendinosus muscles (Figure S1). In individual 1, muscle CT was performed in her most advanced stage of NM. Muscles were diffusely atrophic. Proximal-dominant muscle atrophy was recognized in her legs (Figure S2).

Histological examination of biopsied muscles from the four showed similar characteristics: mild to moderate variation in myofiber size and nemaline bodies with a granular shape in scattered muscle fibers on modified Gomori trichrome staining (Figures 2A and 2B). In individual 1, muscle fibers were decreased in number with extensive fat replacement and increased connective tissue proliferation. Intranuclear nemaline rods were observed in individuals 1 and 4 (Figures 2B and 2C). Type 1 fiber predominance, which is commonly seen in congenital myopathies, was confirmed on myosin ATPase staining in all four individuals (data not shown). Electron microscopy (EM) confirmed the presence of nemaline bodies in all three individuals examined (Figure 2C).

We first genetically analyzed individual 1. Because of the intranuclear rods in her biopsied muscle, we searched for ACTA1 abnormality by Sanger sequencing but failed to detect a mutation. Considering an autosomal-recessive mode of inheritance given the consanguinity, we performed homozygosity mapping and identified six homozygously stretched regions with a total size of 47.6 Mb

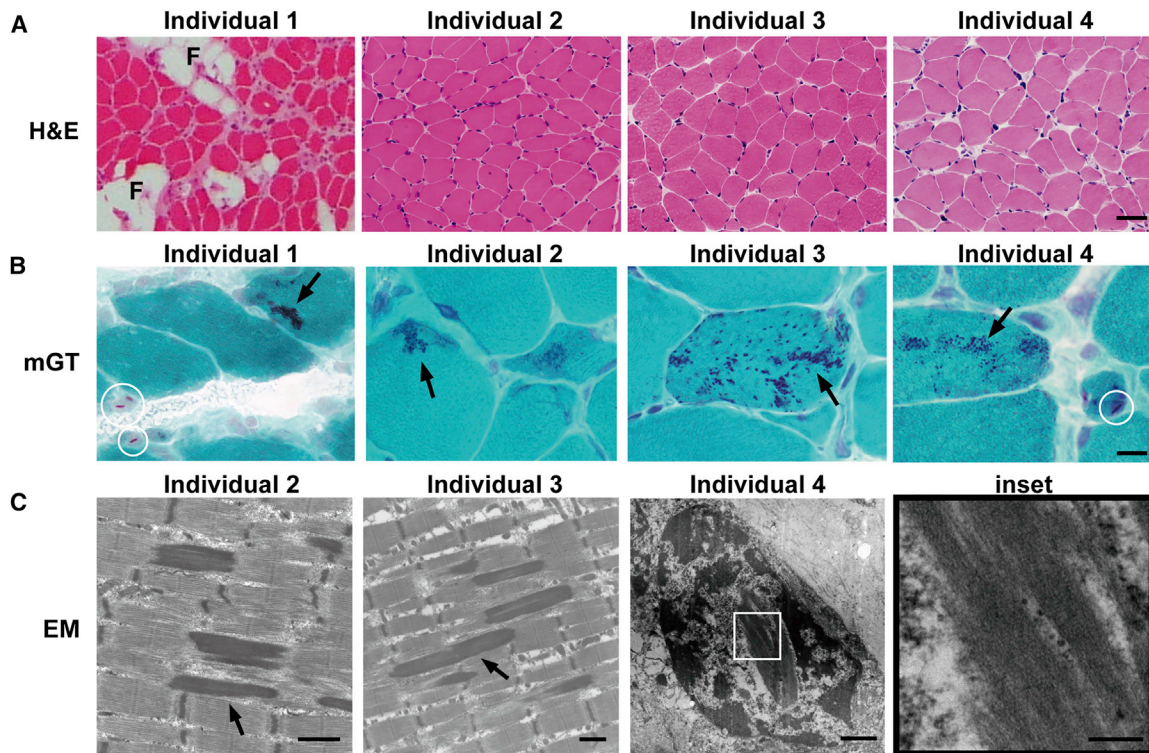


Figure 2. Pathologies of Biopsied Muscle from the Studied Individuals

For muscle histology, the muscle samples were frozen in liquid-nitrogen-cooled isopentane and stored at -80°C . They were then sectioned at a thickness of $10\ \mu\text{m}$ and exposed to a battery of routine histochemical stains, including hematoxylin and eosin (H&E), modified Gomori trichrome (mGT), and NADH-TR.¹⁵ Regarding the method of electron microscopy (EM), see the [Figure S7](#) legend. Because we could not obtain standard EM samples of the muscles from individual 4, frozen sections were fixed with 2.5% glutaraldehyde in cacodylate buffer and subjected to standard epon-embedded EM block preparation.

(A) Sections stained with H&E show marked variation in fiber size, including replacement of interstitial connective and fat (F) tissue in individual 1, who is wheelchair bound. The other three individuals showed mild to moderate variation in fiber size with scattered small angular fibers representative of mild muscle changes. No apparent degenerative changes were recognized. Scale bar represents $50\ \mu\text{m}$.

(B) mGT staining of biopsied muscle. Scattered fibers containing dispersed to aggregated darkly stained nemaline bodies in the cytoplasm (arrows) were found in all subjects. Most of the bodies were round and not rod-like in shape. Intranuclear rods (encircled) with a fine string-like appearance (stained red) were seen in individuals 1 and 4. Scale bar represents $10\ \mu\text{m}$.

(C) EM confirmed the presence of nemaline bodies (arrow) with the same electron density as the Z-line in individuals 2 and 3. Most of the bodies were short and rarely longer than the length of one sarcomere. Note the relatively well-preserved myofibrils. An intranuclear rod was seen in individual 4; it had a slightly lower electron density than intracytoplasmic nemaline bodies but a lattice-like structure (inset). Scale bar represents $1\ \mu\text{m}$.

([Figure S3](#) and [Table S1](#)). Then, we performed whole-exome sequencing (WES) of the proband's DNA obtained from her saliva by using OrageneDNA (DNA Genotek) as previously described.¹⁶ In brief, genomic DNA was captured with a SureSelect Human All Exon V4 Kit (Agilent Technologies) and sequenced on an Illumina HiSeq 2000 with 101-bp paired-end reads. Reads were aligned to GRCh37 with Novoalign. PCR duplicates were removed with Picard. Local realignments around indels and base quality-score recalibration were performed with the Genome Analysis Toolkit (GATK). Variants were called by the GATK UnifiedGenotyper and filtered on the basis of the GATK Best Practices (version 3). The common variants registered in dbSNP135 (minor allele frequency ≥ 0.01) and not flagged as having clinical associations were excluded. Variants that passed the filtering steps were annotated with ANNOVAR.¹⁷ The mean depth of coverage against the RefSeq coding sequence by WES was $102\times$, and

94% of the total coding sequence was covered by ten reads or more. We obtained 359 rare protein-altering and splice-site variants, which were not observed in more than 5 of 575 in-house control exomes. WES did not identify any pathogenic mutation in *ACTA1* or nine other genes associated with NM. Homozygous *MYPN* c.2003delA (GenBank: NM_032578.3), which is predicted to result in p.Asn668Thrfs*25, was the only homozygous mutation located in the homozygous regions. Sanger sequencing confirmed the *MYPN* mutation ([Figure 1B](#)).

MYPN encodes myopalladin (MYPN), a 145-kDa multifunctional protein localized at sarcomere Z- and I-bands, as well as at the nucleus of cardiac and skeletal myocytes.^{18,19} The primary structure of MYPN consists of five immunoglobulin (Ig) domains (Ig domains 1 and 2 at the N terminus and Ig domains 3–5 at the C terminus). The C-terminal and central regions of MYPN bind to α -actinin and nebulin (skeletal muscle) or nebulin (cardiac muscle)

at the Z-line (Figure S4). MYPN- α -actinin-nebulin can form a link tethering actin thin filaments and titin filaments within the Z-line, thus assembling I-Z-I bodies in striated muscle.^{18,19} Notably, mutations in *NEB* (MIM: 161650), encoding nebulin, are the most common cause of NM. The N-terminal region of MYPN binds to cardiac ankyrin repeat protein (CARP, also known as ankyrin repeat domain-containing protein 1 [ANKRD1]), attached to titin at the I-band.¹⁸ CARP is a multifunctional protein that is not only a component of the sarcomere but also a transcription cofactor in the nucleus.²⁰ CARP has dual intracellular localization in the sarcomere and nucleus, and MYPN shuttles (colocalizes) with CARP in the nucleus.¹⁸

After finding a homozygous *MYPN* mutation in individual 1, we performed further WES studies by using a HiSeq 1000 (Illumina) in 54 additional genetically unsolved families affected by histologically diagnosed NM in biopsied muscles. This cohort included individuals with relatively mild, later-onset forms of NM: mean and median ages of onset were 25 and 26 years, respectively. No possible variants in genes known to be associated with congenital myopathy were detected by either target resequencing or WES in this cohort (Table S2). Genomic DNA was extracted from either peripheral-blood leukocytes or biopsied muscle and then subjected to solution capture with the SureSelect Human All Exon V5 Kit (Agilent Technologies) for the generation of barcoded WES libraries. These libraries were sequenced on an Illumina HiSeq 1000 with paired-end 100-bp reads. The mean depths of coverage by WES for subjects 2, 3, and 4 were 69 \times , 97 \times , and 111 \times , respectively, and 90%, 95%, and 99%, respectively, of the total coding sequence was covered by ten reads or more. Alignment, variant calling, and annotation were performed with the Burrows-Wheeler Aligner,²¹ Picard, GATK, and ANNOVAR. As predicted, we identified three more biallelic truncating mutations in *MYPN* in individuals 2–4; all of these mutations were confirmed by Sanger sequencing (Figure 1B). Individual 2 had a homozygous splice-acceptor-site mutation (c.3076–2A>C). Individual 3 had a homozygous nonsense mutation (c.1129C>T) leading to p.Arg377*. Individual 4 had compound-heterozygous nonsense mutations c.[3169C>T];[3214C>T], resulting in p.[Arg1057*];[Arg1072*]. Compound heterozygosity was confirmed through DNA analyses of the parents. All mutations except for c.1129C>T were absent from publicly available human variation resources (the Human Genetic Variation Database [HGVD], which holds exome data from 1,208 normal Japanese control individuals,²² the NHLBI Exome Sequencing Project Exome Variant Server [ESP6500], and the Exome Aggregation Consortium [ExAC] Browser). The c.1129C>T variant was present only in the ExAC Browser with extremely low frequency (0.000008246), such that it was in a heterozygous state (Table S3) in only 1 of 66,674 alleles registered from a non-Finnish European population. No pathogenic mutation in known NM-associated genes was found in these three individuals. Therefore, we concluded that 3 of the 54 families (5.6%) in our NM cohort had mutations in *MYPN*.

Because individual 2 had a homozygous splice-acceptor-site mutation (c.3076–2A>C), we analyzed cDNA by using total RNA extracted from the biopsied muscle. Four aberrant transcripts were identified: complete inclusion of intron 14 with substitution of r.3076–2A>C (r.[3076–2A>C;3075_3076ins3075+1_3076–1]), deletion of the first five bases of exon 15 (r.3076_3080del), deletion of the first 11 bases of exon 15 (r.3076_3086del), and skipping of exon 15 after the deletion of the first 73 bases of exon 16 (r.3076_3231del). The first three transcripts resulted in a truncated MYPN (p.Gly1026Valfs*21, p.Gly1026Asnfs*59, and p.Gly1026Leufs*57), which might undergo nonsense-mediated mRNA decay (NMD). The fourth transcript, which was observed scarcely, resulted in the deletion of 52 amino acids of MYPN (p.Gly1026_Gln1077del), which might disrupt Ig domains 3 and 4 and remove the α -actinin binding region, thus probably leading to functional impairment (Figure S5).

We undertook further protein analyses on frozen biopsied biceps brachii muscles, which we obtained from individuals 2–4. Because the biopsied muscle sample was depleted in individual 1, we converted skin fibroblasts into myotubes by using adenovirus-mediated *MYOD1* (MIM: 159970) expression as previously described.^{23–25} Immunohistochemistry of muscles from individuals 2–4 with the use of anti-MYPN antibody (HPA036298, Atlas Antibodies) and anti- α -actinin (EA-53, Sigma-Aldrich) revealed that MYPN was not stained in the affected myofibers, whereas MYPN colocalized with α -actinin at the Z-line in control muscle (Figure 3A). Western blotting performed with anti-MYPN antibody and anti- α -tubulin (DM1A, Sigma-Aldrich) showed that full-length MYPN was undetectable in transdifferentiated myotubes of individual 1 and the muscles of individuals 2–4 (Figures 3B and 3C). These findings suggest that the nonsense and splice-site mutations markedly decrease MYPN levels. Given its interaction with sarcomeric components, the absence of MYPN might affect the maintenance of sarcomeric structure and lead to NM (Figure S4). Considering the interaction between MYPN and nebulin, we performed nebulin immunohistochemical analysis by using skeletal muscles from individuals 3 and 4 and anti-nebulin (N-9891, Sigma-Aldrich) and anti- α -actinin (ab137346, Abcam). Nebulin retained its normal localization between the Z-lines (α -actinin staining), and we did not see any alteration in comparison to that in control tissues (Figure S6). Furthermore, we measured the actin filament length of individuals 2 and 3 and control individuals by phalloidin staining and/or EM. Actin filament length did not show any obvious alteration in individual 2 or 3 (Figure S7).

To date, 24 monoallelic heterozygous mutations in *MYPN* have been reported to cause hypertrophic cardiomyopathy (MIM: 615248), dilated cardiomyopathy (DCM [MIM: 615248]), restrictive cardiomyopathy (RCM [MIM: 615248]), sudden arrhythmic death syndrome, or sudden unexpected death in infancy with incomplete penetrance (as of October 2, 2016) (Figure S8).^{19,26–28} These include

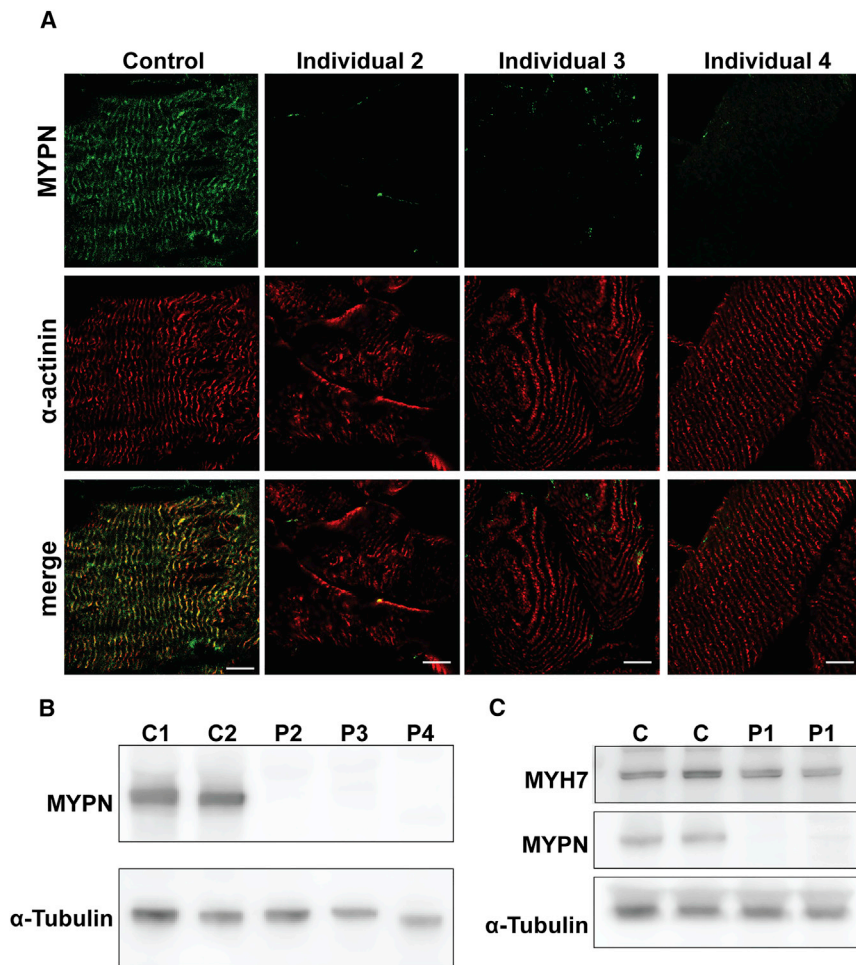


Figure 3. Immunohistological and Protein Analyses of the Studied Individuals

(A) Immunohistochemical staining was performed on 10- μ m-thick frozen sections of muscles with a rabbit polyclonal anti-MYPN antibody, mouse monoclonal anti- α -actinin (EA-53; Sigma-Aldrich), and DAPI (Wako). Each section was observed under a fluorescence microscope, LSM710 (Zeiss), with Zen software (Zeiss). Immunohistochemical staining showed colocalization of MYPN and α -actinin in control skeletal muscle. In individuals 2–4, MYPN was not stained, whereas α -actinin showed a normal striated staining pattern. Scale bars represent 10 μ m.

(B) Each muscle sample was lysed with SDS sample buffer (125 mM Tris-HCl [pH 6.8], 5% 3-mercapto-1,2-propanediol, 2% SDS, and 10% glycerol) and then subjected to western blotting on a NuPAGE 3%–8% Tris-acetate gel (Thermo Fisher Scientific).¹⁵ The primary antibodies used were rabbit polyclonal anti-MYPN (HPA036298; Atlas Antibodies) and mouse monoclonal anti- α -tubulin (DM1A; Sigma-Aldrich). After incubation with secondary antibody, polyvinylidene difluoride membrane was developed with Amersham ECL Western Blotting Detection Reagents (GE Healthcare Life Sciences). Full-length MYPN was not detected in biopsied skeletal muscle from individuals 2–4. α -Tubulin was used as a loading control. Abbreviations are as follows: C1, control 1; C2, control 2; P2, individual 2; P3, individual 3; and P4, individual 4.

(C) Western blotting of transdifferentiated myotubes with adenoviral-mediated

MYOD1 expression detected MYPN in control cells. A myoblast from individual 1 did not show MYPN. Myosin heavy chain 7 (MYH7) was used as a skeletal muscle differentiation marker, and α -tubulin was used as a loading control. Abbreviations are as follows: C, control; and P1, individual 1.

21 missense mutations,^{19,26,29–31} two nonsense mutations,¹⁹ and one 1-bp deletion,²⁶ and most of them were suspected to have dominant-negative effects (Figures S8 and S9, row 2).^{19,26,32} Among the three possible truncating mutations, two (c.1585C>T [p.Gln529*] and c.2653C>T [p.Arg885*]) are located within the 50-bp region upstream of each exon junction, implying the possible escape from NMD, and the truncated MYPN might cause the dominant-negative effect. Only one individual with DCM and c.248delT (p.Ile83Thrfs*23) in *MYPN* has been reported, and haploinsufficiency was suspected as a possible causative mechanism according to expression analysis.²⁶ Considering the incomplete penetrance of the mutation in the family (two asymptomatic subjects with the mutation),²⁶ it is difficult to draw definitive conclusions on its pathogenicity in cardiomyopathy.

In the case of heterozygous c.1585C>T (p.Gln529*) in *MYPN*, it was experimentally confirmed that it escapes NMD and produces a truncated 65-kDa MYPN by acting as a “poison peptide” to disrupt Z-band organization.^{19,32} The phenotype of knockin mutant mice harboring a heterozygous *MYPN* p.Gln526* variant (*MYPN*^{WT/Gln526*}),

equivalent to human heterozygous c.1585C>T in *MYPN*, was associated with RCM.³² Mutant mice with a homozygous *MYPN* p.Gln526* variant (*MYPN*^{Gln526*}) displayed impaired *Mypn* transcription in heart and skeletal muscle.³² Thus, assuming that the *MYPN*^{Gln526*} mice can be considered a *Mypn*-null model, we analyzed the skeletal muscle samples of 3-month-old *MYPN*^{Gln526*} mice as a model of human NM. *MYPN*^{WT/Gln526*} mice and wild-type (WT) littermates of the same age were used as controls. We confirmed by western blotting that truncated MYPN was not detected in skeletal muscle from homozygous mice (data not shown). As previously reported, no apparent abnormalities were recognized in skeletal muscles from either homozygous mutants or WT mice on hematoxylin and eosin and modified Gomori staining (Figure 4A).³² Western blotting revealed the presence of full-length MYPN in WT and heterozygous mutants, but not in homozygous ones (Figure 4B). On EM, Z-streaming and small nemaline-like bodies were observed in homozygous mice, whereas well-organized sarcomeres were seen in heterozygous and WT ones, implying the presence of mild NM in the homozygotes (Figure 4C). Although EM showed

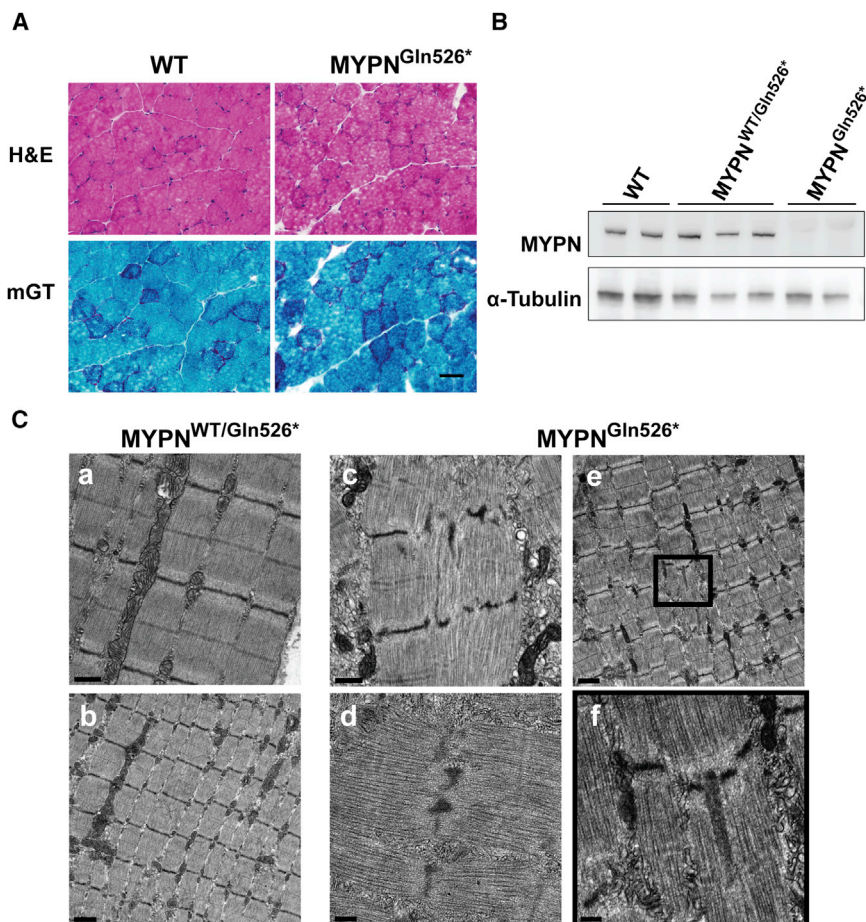


Figure 4. Skeletal Muscle Studies of Knockin Mice with Heterozygous and Homozygous Nonsense Mutations in *MyoD*

(A) No apparent abnormality was observed in skeletal muscles of wild-type (WT) mice or mutant mice carrying a homozygous *MYPN* p.Gln526* variant (*MYPN*^{Gln526*}) on H&E and mGT. Scale bar represents 50 μ m.

(B) Western blotting of *MYPN* for wild-type (WT), heterozygous (*MYPN*^{WT/Gln526*}), and homozygous (*MYPN*^{Gln526*}) mice. In homozygous mice, full-length or truncated *MYPN* was not detected. α -Tubulin was used as a loading control.

(C) EM of heterozygous (*MYPN*^{WT/Gln526*}) and homozygous (*MYPN*^{Gln526*}) mice. In heterozygous mice, no abnormality in the Z-line was seen. In homozygous mice, Z-line streaming (c) and thickening (d) were observed. In addition, there was a tiny nemaline-like structure that continued from the Z-line (e, inset). Scale bars represent 0.5 μ m (a), 1 μ m (b), 0.5 μ m (c), 0.2 μ m (d), 1 μ m (e), and 0.2 μ m (f).

NM with full penetrance but mild cardiomyopathy with low penetrance (Figure S9, row 3), and (3) heterozygous loss-of-function mutations might be generally associated with no phenotypic disruption in either skeletal or cardiac muscle. We could not completely rule out the possible

mild Z-line abnormality in homozygous mice, muscle weakness was not detected in them, perhaps replicating NM compatible with the mild NM phenotype in humans.³² However, we do not rule out the possibility that muscle weakness appears in homozygous mice at a later stage.

Given that individual 1 has presented with cardiac hypertrophy since 12 years of age and individual 4 exhibits a hypokinetic heart, we assumed that these mutations might also be associated with mild cardiomyopathy. Thus, parents of individual 4 underwent a chest X-ray, electrocardiogram, and echocardiogram. These examinations revealed no cardiac involvement, implying that haploinsufficiency of these *MYPN* mutations might not be sufficiently detrimental to disrupt the maintenance of cardiac muscle sarcomeres. In addition, pathological changes in cardiac muscle might differ between those carrying a heterozygous dominant-negative *MYPN* mutation and those with biallelic loss-of-function *MYPN* mutations, depending on the different molecular mechanisms between them. To clarify this concept, we propose a possible model based on mutation types, zygosity, phenotype, and penetrance as follows: (1) heterozygous dominant-negative *MYPN* mutations might be associated with cardiomyopathy with incomplete penetrance (Figure S9, row 2), (2) biallelic loss-of-function mutations might be associated with

association between a heterozygous loss-of-function mutation and cardiomyopathy because of one previously reported family (Figure S9, row 4).

This study identified biallelic loss-of-function *MYPN* mutations in 3 of 54 families with undiagnosed NM as one cohort. NM was classified into six categories according to age of onset and clinical severity,³³ and congenital, childhood, and adult onsets constitute 82%, 13%, and 4% of NM, respectively.¹³ Our cohort includes individuals with differing onset ages of histologically diagnosed NM for which the genetic cause had not been previously resolved. Consequently, our cohort could include more individuals with childhood or adult onset than other previously reported cohorts,¹³ leading us to identify *MYPN* mutations at a relatively high rate. Thus, biallelic *MYPN* mutations could be relatively common in later-onset NM. In the ExAC Browser, 14 truncating variants with high sequencing quality have been registered. The allele frequency in each ethnicity from which each variant was found ranged from $\sim 1.5 \times 10^{-5}$ (c.3158+1G>A; 1/66,678 alleles in non-Finnish Europeans) to $\sim 2.3 \times 10^{-4}$ (c.3796C>T [p.Gln1266*]; 2/8,654 alleles in East Asians) without any homozygotes. If we assume the incidence of NM to be 1:50,000 live births,² approximately 1.8% of all individuals with NM might be explained by the biallelic *MYPN* truncating mutations given their allele frequencies

(Table S4). However, larger studies are needed to confirm this estimation.

Common NM features associated with these biallelic *MYPN* mutations seemed to include a relatively mild form and relatively small and round nemaline bodies in biopsied muscle in comparison with those in other genetically confirmed forms of NM. In addition, EM did not show disorganized myofibrils in the affected individuals, which is compatible with a mild phenotype. One possible hypothesis for this mild phenotype is that it might be associated with the compensation for the absence of *MYPN* by another protein that is highly homologous to it, namely, palladin, which is ubiquitously localized, especially in striated and smooth muscles.¹⁸ In striated muscle, palladin colocalizes with α -actinin at the Z-line and is required for normal organization of the actin cytoskeleton.³⁴ It was also predicted that palladin's three Ig domains interact with α -actinin at the C terminus.¹⁸ Whereas high (62.7%) sequence identity between *MYPN* and palladin has been identified in the α -actinin-nebulin-binding region, relatively low sequence homology has been noted within the CARP-binding region at the N terminus (Figure S10). In contrast to palladin, *MYPN* has a dual role as a component of the sarcomere localizing at the Z- and I-bands and as a regulator of gene expression by interacting with CARP, which localizes in the nucleus. Thus, palladin might provide only partial compensation for *MYPN*, potentially leading to the mild phenotype seen in NM. In knockin mutant mice harboring either the heterozygous or homozygous *MYPN*-p.Gln526* variant, palladin was found to be present in the heart of both mutants.³² Using western blotting, we examined the level of palladin in skeletal muscles available from individuals 3 and 4. We confirmed that the level of palladin in biopsied muscles did not differ between affected and control individuals (Figure S11).

Another explanation for the mild phenotype of *MYPN*-associated NM could be related to different expression timelines of the two genes *PALLD* (MIM: 608092; encoding palladin) and *MYPN*. Palladin, not *MYPN*, was detected in the earliest I-Z-I bodies as a Z-line precursor, and then it might be partially replaced by *MYPN* during myofibril assembly.¹⁸ Recently, it was also reported that palladin promotes correct myoblast proliferation at an early developmental stage and later allows myoblasts to differentiate into mature myofibers.³⁵ We assume that palladin in the developmental stage of the initial formation of myofibers might functionally complement biallelic *MYPN* mutations, whereas symptoms appear after the replacement of palladin by *MYPN*.

Recently, part of the disease mechanism for NM has been revealed through studies on skeletal muscle development and its force generation in humans.² It was reported that lower force generation was observed in muscles from NM associated with all eight known genes tested (*NEB*, *ACTA1*, *TPM3*, *TPM2*, *TNNT1*, *KBTBD13*, *KLHL40*, and *KLHL41*),³⁶ implying that this could be a commonly

observed finding in NM. Among them, abnormally shorter thin filament lengths were associated with reduced force generation in *NEB*- and *ACTA1*-related NM.³⁶ In another report, some of the mutations in *TPM2* (encoding tropomyosin) changed the protein conformation and the affinity for thin filament or affected calcium activation for contractility, all of which might lead to muscle weakness.³⁷ Our protein studies suggest that there might be a mechanism for possible lower force generation other than shorter thin filaments, impaired nebulin, or α -actinin localization. Further functional studies are needed to elucidate decreased force generation regarding contractile dynamics and calcium handling in *MYPN*-related NM.

In conclusion, we have shown that biallelic loss-of-function mutations in *MYPN* in four families are associated with childhood- to adult-onset, slowly progressive NM, which extends our knowledge of the genetic heterogeneity of NM. We emphasize that unique characteristics of *MYPN*-related NM, such as mild, slowly progressive motor symptoms, possible cardiac problems, and intranuclear rods in biopsied skeletal muscle samples, could be used as clinical markers of this disease and indications for *MYPN* screening.

Supplemental Data

Supplemental Data include a Supplemental Note, Supplemental Acknowledgments, 11 figures, and 4 tables and can be found with this article online at <http://dx.doi.org/10.1016/j.ajhg.2016.11.017>.

Acknowledgments

We thank all of the participants for their cooperation in this research. We also thank Dr. M. Takeuchi (Department of Neurology, Neurological Institute, Tokyo Women's Medical University) for preparing biopsied muscle samples and Prof. S. Labeit (Department of Integrative Pathophysiology, Medical Faculty Mannheim, University of Heidelberg) and Prof. A. Kimura and Dr. T. Arimura (Department of Molecular Pathogenesis, Division of Pathophysiology, Medical Research Institute, Tokyo Medical and Dental University) for their kind gift of the *MYPN* antibody. We also thank Dr. K. Takagi (Department of Pediatrics, Jikei University) for his collaboration in the mouse study. We are also grateful to Mr. T. Miyama, Ms. K. Takabe, Ms. N. Watanabe, Ms. S. Sugimoto, Mr. S. Nakamura, and Ms. M. Sato (Department of Human Genetics, Yokohama City University Graduate School of Medicine); Ms. H. Kunimoto, Ms. S. Yoshida, Ms. Y. Tsutsumi, Ms. K. Ishikawa, Ms. C. Miyazaki, Ms. M. Arai, Ms. A. Oda, Ms. K. Tatezawa, Mr. H. Nakamura, and Ms. M. Ogawa (Department of Neuromuscular Research, National Institute of Neuroscience, NCNP); and Mr. N. Miyata (Department of Genome Medicine Development, Medical Genome Center, NCNP) for their technical assistance. The grants that supported this study are listed in the Supplemental Acknowledgments.

Received: August 7, 2016

Accepted: November 22, 2016

Published: December 22, 2016

Web Resources

ANNOVAR, <http://annovar.openbioinformatics.org/en/latest/dbSNP>, <http://www.ncbi.nlm.nih.gov/SNP/>
ExAC Browser, <http://exac.broadinstitute.org/>
Genome Analysis Toolkit (GATK), <https://www.broadinstitute.org/gatk/>
HomozygosityMapper, <http://www.homozygositymapper.org/>
Human Genetic Variation Database, <http://www.genome.med.kyoto-u.ac.jp/SnpDB/>
MutationTaster, <http://www.mutationtaster.org/>
NHLBI Exome Sequencing Project (ESP) Exome Variant Server, <http://evs.gs.washington.edu/EVS/>
Novoalign, <http://www.novocraft.com/products/novoalign/>
OMIM, <http://www.omim.org/>
Picard, <http://broadinstitute.github.io/picard/>
PolyPhen2, <http://genetics.bwh.harvard.edu/pph2/>
Primer3, <http://bioinfo.ut.ee/primer3-0.4.0/>
RefSeq, <http://www.ncbi.nlm.nih.gov/refseq/>
SIFT, <http://sift.jcvi.org/>
UCSC Human Genome Browser, <https://genome.ucsc.edu/>

References

1. Nance, J.R., Dowling, J.J., Gibbs, E.M., and Bönnemann, C.G. (2012). Congenital myopathies: an update. *Curr. Neurol. Neurosci. Rep.* *12*, 165–174.
2. Romero, N.B., Sandaradura, S.A., and Clarke, N.F. (2013). Recent advances in nemaline myopathy. *Curr. Opin. Neurol.* *26*, 519–526.
3. Nowak, K.J., Wattanasirichaigoon, D., Goebel, H.H., Wilce, M., Pelin, K., Donner, K., Jacob, R.L., Hübner, C., Oexle, K., Anderson, J.R., et al. (1999). Mutations in the skeletal muscle alpha-actin gene in patients with actin myopathy and nemaline myopathy. *Nat. Genet.* *23*, 208–212.
4. Pelin, K., Hilpelä, P., Donner, K., Sewry, C., Akkari, P.A., Wilton, S.D., Wattanasirichaigoon, D., Bang, M.L., Centner, T., Hanefeld, F., et al. (1999). Mutations in the nebulin gene associated with autosomal recessive nemaline myopathy. *Proc. Natl. Acad. Sci. USA* *96*, 2305–2310.
5. Laing, N.G., Wilton, S.D., Akkari, P.A., Dorosz, S., Boundy, K., Kneebone, C., Blumbergs, P., White, S., Watkins, H., Love, D.R., et al. (1995). A mutation in the alpha tropomyosin gene TPM3 associated with autosomal dominant nemaline myopathy NEM1. *Nat. Genet.* *10*, 249.
6. Donner, K., Ollikainen, M., Ridanpää, M., Christen, H.J., Goebel, H.H., de Visser, M., Pelin, K., and Wallgren-Pettersson, C. (2002). Mutations in the beta-tropomyosin (TPM2) gene—a rare cause of nemaline myopathy. *Neuromuscul. Disord.* *12*, 151–158.
7. Johnston, J.J., Kelley, R.I., Crawford, T.O., Morton, D.H., Agarwala, R., Koch, T., Schäffer, A.A., Francomano, C.A., and Biesecker, L.G. (2000). A novel nemaline myopathy in the Amish caused by a mutation in troponin T1. *Am. J. Hum. Genet.* *67*, 814–821.
8. Agrawal, P.B., Greenleaf, R.S., Tomczak, K.K., Lehtokari, V.L., Wallgren-Pettersson, C., Wallefeld, W., Laing, N.G., Darras, B.T., Maciver, S.K., Dormitzer, P.R., and Beggs, A.H. (2007). Nemaline myopathy with minicores caused by mutation of the CFL2 gene encoding the skeletal muscle actin-binding protein, cofilin-2. *Am. J. Hum. Genet.* *80*, 162–167.
9. Yuen, M., Sandaradura, S.A., Dowling, J.J., Kostyukova, A.S., Moroz, N., Quinlan, K.G., Lehtokari, V.L., Ravenscroft, G., Todd, E.J., Ceyhan-Birsoy, O., et al. (2014). Leiomodlin-3 dysfunction results in thin filament disorganization and nemaline myopathy. *J. Clin. Invest.* *124*, 4693–4708.
10. Sambuughin, N., Yau, K.S., Olivé, M., Duff, R.M., Bayarsaikhan, M., Lu, S., Gonzalez-Mera, L., Sivadurai, P., Nowak, K.J., Ravenscroft, G., et al. (2010). Dominant mutations in KBTBD13, a member of the BTB/Kelch family, cause nemaline myopathy with cores. *Am. J. Hum. Genet.* *87*, 842–847.
11. Ravenscroft, G., Miyatake, S., Lehtokari, V.L., Todd, E.J., Vornanen, P., Yau, K.S., Hayashi, Y.K., Miyake, N., Tsurusaki, Y., Doi, H., et al. (2013). Mutations in KLHL40 are a frequent cause of severe autosomal-recessive nemaline myopathy. *Am. J. Hum. Genet.* *93*, 6–18.
12. Gupta, V.A., Ravenscroft, G., Shaheen, R., Todd, E.J., Swanson, L.C., Shiina, M., Ogata, K., Hsu, C., Clarke, N.F., Darras, B.T., et al. (2013). Identification of KLHL41 Mutations Implicates BTB-Kelch-Mediated Ubiquitination as an Alternate Pathway to Myofibrillar Disruption in Nemaline Myopathy. *Am. J. Hum. Genet.* *93*, 1108–1117.
13. Ryan, M.M., Schnell, C., Strickland, C.D., Shield, L.K., Morgan, G., Iannaccone, S.T., Laing, N.G., Beggs, A.H., and North, K.N. (2001). Nemaline myopathy: a clinical study of 143 cases. *Ann. Neurol.* *50*, 312–320.
14. Laing, N.G., Dye, D.E., Wallgren-Pettersson, C., Richard, G., Monnier, N., Lillis, S., Winder, T.L., Lochmüller, H., Graziano, C., Mitrani-Rosenbaum, S., et al. (2009). Mutations and polymorphisms of the skeletal muscle alpha-actin gene (ACTA1). *Hum. Mutat.* *30*, 1267–1277.
15. Mitsushashi, S., Hatakeyama, H., Karahashi, M., Koumura, T., Nonaka, I., Hayashi, Y.K., Noguchi, S., Sher, R.B., Nakagawa, Y., Manfredi, G., et al. (2011). Muscle choline kinase beta defect causes mitochondrial dysfunction and increased mitophagy. *Hum. Mol. Genet.* *20*, 3841–3851.
16. Saitsu, H., Nishimura, T., Muramatsu, K., Kodera, H., Kumada, S., Sugai, K., Kasai-Yoshida, E., Sawaura, N., Nishida, H., Hoshino, A., et al. (2013). De novo mutations in the autophagy gene WDR45 cause static encephalopathy of childhood with neurodegeneration in adulthood. *Nat. Genet.* *45*, 445–449, e1.
17. Wang, K., Li, M., and Hakonarson, H. (2010). ANNOVAR: functional annotation of genetic variants from high-throughput sequencing data. *Nucleic Acids Res.* *38*, e164.
18. Bang, M.L., Mudry, R.E., McElhinny, A.S., Trombitás, K., Geach, A.J., Yamasaki, R., Sorimachi, H., Granzier, H., Gregorio, C.C., and Labeit, S. (2001). Myopalladin, a novel 145-kilodalton sarcomeric protein with multiple roles in Z-disc and I-band protein assemblies. *J. Cell Biol.* *153*, 413–427.
19. Purevjav, E., Arimura, T., Augustin, S., Huby, A.C., Takagi, K., Nunoda, S., Kearney, D.L., Taylor, M.D., Terasaki, F., Bos, J.M., et al. (2012). Molecular basis for clinical heterogeneity in inherited cardiomyopathies due to myopalladin mutations. *Hum. Mol. Genet.* *21*, 2039–2053.
20. Zou, Y., Evans, S., Chen, J., Kuo, H.C., Harvey, R.P., and Chien, K.R. (1997). CARP, a cardiac ankyrin repeat protein, is downstream in the Nkx2-5 homeobox gene pathway. *Development* *124*, 793–804.
21. Li, H., and Durbin, R. (2009). Fast and accurate short read alignment with Burrows-Wheeler transform. *Bioinformatics* *25*, 1754–1760.
22. Higasa, K., Miyake, N., Yoshimura, J., Okamura, K., Niihori, T., Saitsu, H., Doi, K., Shimizu, M., Nakabayashi, K., Aoki, Y., et al.

- (2016). Human genetic variation database, a reference database of genetic variations in the Japanese population. *J. Hum. Genet.* *61*, 547–553.
23. Nozawa, R.S., Nagao, K., Igami, K.T., Shibata, S., Shirai, N., Nozaki, N., Sado, T., Kimura, H., and Obuse, C. (2013). Human inactive X chromosome is compacted through a PRC2-independent SMCHD1-HBiX1 pathway. *Nat. Struct. Mol. Biol.* *20*, 566–573.
 24. Ugai, H., Murata, T., Nagamura, Y., Ugawa, Y., Suzuki, E., Nakata, H., Kujime, Y., Inamoto, S., Hirose, M., Inabe, K., et al. (2005). A database of recombinant viruses and recombinant viral vectors available from the RIKEN DNA bank. *J. Gene Med.* *7*, 1148–1157.
 25. Fukuda, H., Terashima, M., Koshikawa, M., Kanegae, Y., and Saito, I. (2006). Possible mechanism of adenovirus generation from a cloned viral genome tagged with nucleotides at its ends. *Microbiol. Immunol.* *50*, 643–654.
 26. Duboscq-Bidot, L., Xu, P., Charron, P., Neyroud, N., Dilanian, G., Millaire, A., Bors, V., Komajda, M., and Villard, E. (2008). Mutations in the Z-band protein myopalladin gene and idiopathic dilated cardiomyopathy. *Cardiovasc. Res.* *77*, 118–125.
 27. Nunn, L.M., Lopes, L.R., Syrris, P., Murphy, C., Plagnol, V., Firman, E., Dalageorgou, C., Zorio, E., Domingo, D., Murday, V., et al. (2016). Diagnostic yield of molecular autopsy in patients with sudden arrhythmic death syndrome using targeted exome sequencing. *Europace* *18*, 888–896.
 28. Hertz, C.L., Christiansen, S.L., Larsen, M.K., Dahl, M., Ferrero-Miliani, L., Weeke, P.E., Pedersen, O., Hansen, T., Grarup, N., Ottesen, G.L., et al. (2016). Genetic investigations of sudden unexpected deaths in infancy using next-generation sequencing of 100 genes associated with cardiac diseases. *Eur. J. Hum. Genet.* *24*, 817–822.
 29. Meyer, T., Ruppert, V., Ackermann, S., Richter, A., Perrot, A., Sperling, S.R., Posch, M.G., Maisch, B., Pankuweit, S.; and German Competence Network Heart Failure (2013). Novel mutations in the sarcomeric protein myopalladin in patients with dilated cardiomyopathy. *Eur. J. Hum. Genet.* *21*, 294–300.
 30. Chami, N., Tadros, R., Lemarbre, F., Lo, K.S., Beaudoin, M., Robb, L., Labuda, D., Tardif, J.C., Racine, N., Talajic, M., and Lettre, G. (2014). Nonsense mutations in BAG3 are associated with early-onset dilated cardiomyopathy in French Canadians. *Can. J. Cardiol.* *30*, 1655–1661.
 31. Zhao, Y., Feng, Y., Zhang, Y.M., Ding, X.X., Song, Y.Z., Zhang, A.M., Liu, L., Zhang, H., Ding, J.H., and Xia, X.S. (2015). Targeted next-generation sequencing of candidate genes reveals novel mutations in patients with dilated cardiomyopathy. *Int. J. Mol. Med.* *36*, 1479–1486.
 32. Huby, A.C., Mendsaikhani, U., Takagi, K., Martherus, R., Wansapura, J., Gong, N., Osinska, H., James, J.F., Kramer, K., Saito, K., et al. (2014). Disturbance in Z-disk mechanosensitive proteins induced by a persistent mutant myopalladin causes familial restrictive cardiomyopathy. *J. Am. Coll. Cardiol.* *64*, 2765–2776.
 33. Wallgren-Pettersson, C., and Laing, N.G. (2000). Report of the 70th ENMC International Workshop: nemaline myopathy, 11–13 June 1999, Naarden, The Netherlands. *Neuromuscul. Disord.* *10*, 299–306.
 34. Parast, M.M., and Otey, C.A. (2000). Characterization of palladin, a novel protein localized to stress fibers and cell adhesions. *J. Cell Biol.* *150*, 643–656.
 35. Nguyen, N.U., and Wang, H.V. (2015). Dual roles of palladin protein in in vitro myogenesis: inhibition of early induction but promotion of myotube maturation. *PLoS ONE* *10*, e0124762.
 36. Winter, J.M., Joureau, B., Lee, E.J., Kiss, B., Yuen, M., Gupta, V.A., Pappas, C.T., Gregorio, C.C., Stienen, G.J., Edvardson, S., et al. (2016). Mutation-specific effects on thin filament length in thin filament myopathy. *Ann. Neurol.* *79*, 959–969.
 37. Marttila, M., Lemola, E., Wallefeld, W., Memo, M., Donner, K., Laing, N.G., Marston, S., Grönholm, M., and Wallgren-Pettersson, C. (2012). Abnormal actin binding of aberrant β -tropomyosins is a molecular cause of muscle weakness in TPM2-related nemaline and cap myopathy. *Biochem. J.* *442*, 231–239.